Received 11 December 2025, accepted 21 February 2026, date of publication 31 March 2026
www.computingonline.net / computing@computingonline.net

Print ISSN 1727-6209
Online ISSN 2312-5381
DOI 10.47839/ijc.25.1.4483

The Influence of Symmetry of Synaptic Connections in MLP on the Values of Object Recognition Metrics

ROMAN PELESHCHAK, VASYL LYTVYN, DMYTRO DOSYN, IVAN PELESHCHAK, TARAS BATIUK

[1]Lviv Polytechnic National University, Lviv, 79013 Ukraine

Corresponding author: Ivan Peleshchak (e-mail: ivan.r.peleshchak@lpnu.ua).

The research was conducted with the grant support of the National Research Foundation of Ukraine "Methods of analysis and optimization of multimodal data for deep learning models in the military sphere", project registration № 2025.07/0017 dated 12.24.2025.

ABSTRACT The paper considers the problem of recognizing objects (anti-tank mines, anti-personnel mines, M14, booby traps) located in soils with different structures (dry sandy, dry calcareous, dry humus, moist sandy, humid and humus, moist calcareous) using MLP with symmetric synaptic connections between neurons of different layers (SMLP) based on data from FLC100 magnetic field sensors with a sensitivity of 10^{-10} – 10^{-4} Tesla. To train the SMLP network, a dataset of fluxgate magnetometer measurements in six soil types was used, divided into training (80%) and test (20%) subsets. The input data is encoded as a three-dimensional vector (voltage, height of the sensor above the ground with a mine, one-hot encoding of 6 soil types). The main difference between SMLP and MLP is the imposition of symmetric constraints on the weight matrix of the second hidden layer, which almost halves the number of synaptic connections between neurons in the hidden layers without significantly degrading recognition quality. The proposed symmetrization mechanism mitigates over-parameterization and overfitting in small-scale magnetometric datasets by introducing structural inductive bias and implicit regularization through symmetry constraints in parameter space. In contrast to convolutional architectures developed for high-dimensional spatial representations, the proposed approach is tailored to structured low-dimensional magnetometric measurements. The MLP and SMLP models were trained for 100 epochs with Adam, RMSprop, and SGD optimizers with a learning rate reduction using ReduceLROnPlateau callback. Experimental results show that SMLP achieves an average accuracy of 99.20% and AUC = 0.9996, which is only 0.09% lower than the traditional MLP (99.29%, AUC = 0.9997), but reduces the training time by 20–30% and behaves more stably under different optimizers. Thus, the SMLP model is productive for use on embedded devices with limited resources.

KEYWORDS passive mine detection; magnetic field sensors; symmetric MLP (SMLP); magnetic anomalies; Adam; RMSprop; SGD.

I. INTRODUCTION

In today's world, the problem of landmines remains one of the most serious threats to the lives of civilians and the recovery of post-conflict territories. Every year, hundreds of people are killed or injured by unexploded ordnance, highlighting the need to develop safe and highly effective methods for detecting and classifying them [1].

Traditional metal detectors detect mines by their metal casings, but modern anti-personnel systems are increasingly being manufactured with minimal or non-metallic casings, which significantly increases the likelihood of missing an explosive device [2]. Active methods, such as radar and ultrasonic systems, although highly sensitive, carry the risk of accidental detonation, which limits their use in the field [3].

In this context, passive mine detection methods based on the analysis of data on magnetic anomalies in their vicinity are gaining increasing attention. In particular, processing fluxgate magnetometer signals using spectral analysis and filtering allows objects to be located beneath the soil surface [4], but these studies did not consider algorithms for classifying mine types and did not take into account the influence of different soil conditions on the signal shape [5].

Some attempts to integrate multilayer perceptrons have shown the promise of MLP for object recognition based on ground-penetrating radar signals, but they were not adapted to magnetometric data and did not use structural constraints of

the network to improve generalization ability [6].

In this work, we propose a new approach for magnetic signal recognition based on MLP with symmetric connections between neurons in hidden layers. Magnetic signals were measured by FLC100 magnetic field sensors [7] with a sensitivity of 10^{-10} – 10^{-4} Tesla in the vicinity of mines located in soils of different structures. Bringing the weight matrix to a symmetric form allows reducing the number of independent parameters, increasing the model's resistance to overfitting, and accelerating the learning process. Similar approaches to network symmetrization have already shown promising results in image and speech signal classification tasks [8].

The aim of the study is to develop an optimized MLP morphology with symmetric connections (SMLP) for high-precision recognition of different types of mines (no mine, anti-tank, anti-personnel, M14, booby trap) in soils of different structures (dry sandy, dry calcareous, dry humus, moist sandy, humid and humus, moist calcareous). In addition, a comparative analysis of the accuracy, learning speed, and noise resistance of standard MLP and symmetric MLP (SMLP) is conducted on a real dataset of magnetic anomalies of different soil types. For this purpose, accuracy, area under the ROC curve (AUC), and loss function indicators are used, as well as model training and inference time.

During a systematic analysis of existing research, we identified several key limitations that hinder further progress in the field of passive mine detection based on magnetometry and the use of neural networks for magnetic signal classification. First of all, many studies focus exclusively on identifying anomalies in the signal without subsequent recognition of mine types. For example, in [4], an in-depth spectral analysis of fluxgate data was performed, which showed high sensitivity to the presence of metal objects, but the study did not build a classification model to distinguish between anti-personnel and anti-tank mines. Similarly, in [5], adaptive filters were proposed to improve the signal-to-noise ratio in heterogeneous soils, but the task of categorization was left unaddressed.

However, these approaches do not provide mine-type recognition based on magnetometric signals. For example, consider multilayer perceptrons with several hidden layers and adaptive weight tuning that takes noise into account, as in [6, 9]. Such models show up to a 5% increase in accuracy, but have only been tested on a limited number of soil environments (mainly sandy and loamy), which does not reflect the diversity of real field conditions.

The third significant drawback is the lack of consideration of structural constraints in networks, which could serve as an additional regularizer and increase the model's ability to generalize. Although weight symmetrization has proven effective in image and time series processing tasks [8, 10], it has not been applied to magnetic signal classification to date. Thus, models without symmetric constraints require more data for training and are less resistant to overfitting.

Another important limitation revealed in recent studies is the insufficient consideration of real measurement noise and non-stationary disturbances in magnetometric signals. In [11], a multiclass classification of UXO based on magnetic field gradients was proposed using classical machine learning classifiers; however, the experiments were carried out under controlled laboratory conditions, which does not reflect real field measurements with strong geomagnetic variations. Similar limitations were observed in [12], where airborne magnetometry combined with deep learning demonstrated high detection accuracy, but the influence of sensor drift and temporal instability of the magnetic background was not sufficiently analyzed.

Several works focus on the integration of UAV-based magnetometric systems for large-area mine detection [13, 14]. These approaches significantly increase the productivity of surveying post-conflict territories; however, the classification stage is often implemented using conventional convolutional neural networks without structural regularization, which limits their generalization in heterogeneous soil environments. In particular, [13] reported up to 91–93% detection accuracy, but the model suffered from a noticeable degradation in performance when transferring to new regions with different soil magnetic properties.

Attempts to use lightweight neural network architectures optimized for embedded systems were presented in [15], where edge computing was applied to airborne magnetometric imaging. Despite the reduction in computational complexity, the models remain sensitive to noise and require large labeled datasets for stable training. This confirms the relevance of introducing additional architectural constraints, such as weight symmetry, to reduce the effective dimensionality of the parameter space.

The problem of low-cost passive magnetic sensing is also actively investigated. In [16], a budget mine detector based on magnetic anomaly analysis was proposed, demonstrating acceptable sensitivity for shallow-buried objects. However, no neural network–based classification was applied, and the system was limited to binary detection. A similar trend is observed in [17], where anisotropic magnetoresistive (AMR) gradiometers were used for mine detection, but the signal processing pipeline relied on threshold-based methods rather than intelligent pattern recognition.

From the standpoint of neural network theory, recent studies confirm the effectiveness of symmetric weight constraints as a powerful form of inductive bias. In [18, 19], symmetric parameterization was applied to deep vision networks and led to improved convergence speed and reduced overfitting. However, none of these works explored the application of symmetry to magnetic signal classification, particularly in the context of passive landmine detection.

Finally, modern approaches increasingly emphasize multimodal data fusion. In [20], optical and magnetometric data integration for UAV-based landmine detection was proposed, achieving robust detection under variable illumination and terrain conditions. Nevertheless, the classification stage remains dominated by conventional CNN-based feature extraction without structural regularization, which once again highlights the gap addressed in the present study.

Since modern methods for improving the quality of object recognition by neural networks increasingly rely on the symmetry of their structures, it is important to develop an MLP architecture with special symmetry constraints that is capable of analyzing complex multidimensional data and accurately classifying landmines with reduced computational resource consumption. Recent studies have demonstrated advanced approaches for dataset optimization and feature extraction that further enhance performance in similar high-complexity tasks [21, 22].

In general, there are several ways to introduce symmetry into the morphology of a neural network. For example,

symmetric convolutional networks with special kernels offer advantages in recognizing mirrored or radially symmetric objects [23], while symmetric activation functions preserve the properties of the network even with significant image distortions [24]. In [25], a convolutional network with diagonalized pooling (DiagPooling) was presented, which demonstrated increased performance compared to classical approaches, and in [26], options for weight symmetry in deep networks were investigated and it was shown that identical or inversely proportional weights located symmetrically relative to the center can improve generalization.

In our work, we address these gaps in three main ways. First, we combined the adaptive signal filtering stage with direct classification by embedding this step into a single pipeline architecture. Second, we expanded the data sample by including samples from minefield experiments in six different soil types (dry sandy, dry calcareous, dry humus, moist sandy, humid and humus, moist calcareous), which allowed us to evaluate the performance of the models in realistic conditions with different noise levels and depths. Third, we integrated a weight symmetrization mechanism in the second hidden layer of the MLP, which allowed us to reduce the number of independent parameters.

The rest of the paper is organized as follows. Section II describes the dataset, preprocessing pipeline, and symmetric weight implementation. Section III presents experimental results, comparative analysis, discusses limitations and future research directions. Section IV concludes the study.

II. MATERIALS AND METHODS

The data source for our study is a publicly available dataset from the Kaggle platform [27], containing magnetic field measurements taken by an FLC100 fluxgate magnetometer in the vicinity of mines at various depths and in six types of soil. This dataset allows us to reproduce real field conditions in which soil moisture and mineral composition change the amplitude and shape of magnetic signals [7, 9].

During the preprocessing stage, artifacts caused by short-term interference and packet loss were removed, and duplicates were excluded. Next, to ensure equal weighting of the channels, normalization was performed, i.e., the mean value for the entire sample was subtracted from each value and divided by the corresponding standard deviation. The original dataset had 339 values, some of which are presented in Table 1 and Table 2. This dataset was augmented to 11,250 samples using the Gaussian noise method. Data augmentation was applied after splitting the dataset into training and test subsets, ensuring that no augmented sample derived from a test instance was included in the training set. This prevents data leakage and artificial inflation of performance metrics. For each selected example x_i, a new example x_i^{new} is generated according to the rule: $x_i^{new} = x_i + \varepsilon$, $\varepsilon \sim N\left(0, \sigma^2 I\right)$, where $x_i \in R^d$ is the original input vector (features) of dimension d (here d=3: V, H, S), $\varepsilon \in R^d$ is a random noise vector, $N\left(0, \sigma^2 I\right)$ is a multivariate normal distribution with a mean of 0 and covariance matrix $\sigma^2 I$, meaning noise is added independently to each feature with equal variance σ^2. I is the identity matrix. The standard deviation of the noise is $\sigma = 0,02$. The original vector $x_i = \left(V_i, H_i, S_i\right)$ is "shifted" in a random direction by a small amount ε, producing a new vector that is similar but not identical.

To evaluate the accuracy of the model, the dataset was divided into training (80% - 9000 values) and test (20% - 2250 values) subsets. After splitting, each of the five classes in the test sample had approximately 450–460 samples (2250 records in total).

In our experiments, we implemented two similar but morphologically different multilayer perceptrons — a standard MLP and its symmetric modification SMLP. Both networks accept a three-dimensional vector consisting of components (V, H, and S) as input.

In our model, the input vector consists of three features, each of which carries experimental information. The first feature, Voltage (V), represents the output voltage of the fluxgate magnetometer, which directly correlates with the magnitude of the local magnetic anomaly caused by a metallic (or non-metallic) object beneath the soil surface. The second feature, Height (H), reflects the height of the sensor above the ground level in centimeters, which is critical for estimating the depth of mines and allows compensating for signal attenuation with increasing distance to the object. The third feature, Soil Type (S), encodes the soil type into 6 categories (dry sandy, dry calcareous, dry humus, moist sandy, humid and humus, moist calcareous), which depend on moisture and particle size distribution and significantly affect the distribution of the magnetic field near the mine. Since Soil Type is a categorical parameter, we use one-hot encoding, obtaining 6 binary variables that indicate the belonging of each measurement to a specific soil type. As a result, each experimental value is fed into the network as a vector: voltage value, height, and soil type indicator [25]. This combination of input data provides a balance between the direct reflection of physical processes and the flexibility of the neural network in working with heterogeneous field measurement conditions.

Table 1. Dependence of fluxgate magnetometer voltage on soil type [15]

Soil	Mine 1 (V)	Mine 2 (V)	Mine 3 (V)	Mine 4 (V)	Mine 5 (V)
1	3,50	10,40	3,80	5,60	3,20
2	3,20	7,70	4,00	5,60	4,40
3	3,50	10,40	6,80	2,60	5,00
4	3,80	10,40	6,50	4,40	5,00
5	3,30	10,40	5,20	2,80	4,40
6	3,32	10,40	5,8	4,3	4,4

Table 1 shows the dependence of the output voltage of a fluxgate magnetometer on soil type for five different mine models. The values for Mine 2 shows a virtually constant amplitude of about 7.8–10.4 V in all soils, while the other models respond in a more differentiated manner: Mine 1 ranges from 3.2 V to 3.8 V, Mine 3 – from 3.8 V to 6.8 V, Mine 4 shows a wide range from 2.6 V to 5.6 V, and Mine 5 – from 3.2 V to 5 V. This table illustrates how soil composition and moisture affect the magnetometer's sensitivity to different types of explosive objects.

Table 2. Dependence of fluxgate magnetometer voltage on Height [15]

Height (cm)	Mine 1 (V)	Mine 2 (V)	Mine 3 (V)	Mine 4 (V)	Mine 5 (V)
0,00	3,70	10,50	4,10	5,80	6,20
1,82	3,50	10,50	4,00	5,60	4,70
3,64	3,48	10,50	3,90	5,00	3,55
5,45	3,20	10,50	3,85	4,40	3,50
7,27	3,05	9,50	3,70	4,30	3,30
9,09	2,80	8,40	3,60	4,25	3,20
10,91	3,05	7,10	3,50	3,90	3,05
12,73	2,80	6,50	3,55	3,70	2,90
14,55	2,60	6,20	3,60	3,50	2,80
16,36	2,85	4,80	3,70	3,20	2,30
18,18	2,87	4,70	3,30	3,10	2,25
20,00	2,50	4,60	3,35	3,00	2,20

Table 2 shows the change in the detected voltage depending on the height of the sensor above the soil surface. For Mine 2, there is a gradual decrease from an initial 10.5 V to approximately 4.6 V, while the other values have more rapid declines: Mine 1 from 3.7 V to 2.5 V, Mine 5 from 6.2 V to 2.2 V, Mine 4 from 5.8 V to 3 V, and Mine 3 from 4.1 V to 3.3 V. This dependence demonstrates how the distance between the sensor and the object affects the amplitude of the magnetic anomaly and emphasizes the importance of taking height into account when modeling the mine detection process.

After the sensory neurons of the input layer, the values (V, H and S) are transmitted to the first hidden layer, which contains sixty-four neurons with ReLU activation and weight initialization. It is this layer that converts the normalized input data into high-level features, using them for more refined processing by the subsequent layers of the network.

The second hidden layer in both models also consists of sixty-four neurons with ReLU. However, in SMLP, we specifically impose a structural symmetry constraint on the weight matrix of the second layer: before the start of each training iteration, weight transformation operations are performed according to the rule $W^{(2)} \to \frac{1}{2}\left(W^{(2)} + \left(W^{(2)}\right)^T\right)$, which guarantees $W_{ij} = W_{ji}$. Thanks to this restriction, the number of independent parameters in this layer is reduced, which contributes to more stable generalization to new data and reduces the risk of overfitting. For the standard MLP, the total number of parameters (including weights and biases) equals 4,741. For the SMLP, due to the imposed symmetry constraint on the 64×64 matrix, the number of independent weights in this layer is reduced from 4,096 to 2,080. As a result, the total number of independent parameters becomes 2,725.

After passing through the last hidden layer, the values from each activation neuron are sent to the output layer with five neurons and a softmax function, which converts the network results into vectors of probabilities of belonging to each of the five classes of soil anomalies with mine hazards. The values of these probabilities are used to calculate losses by categorical cross-entropy (1) and for the accuracy indicator when evaluating the quality of the model.

$$L = -\sum_{i=1}^{C} y_i \log\left(\hat{y}_i\right), \qquad (1)$$

where y_i is the true value (one-hot encoded, i.e., 1 for the correct class and 0 for others), y_i is the predicted probability for class i (softmax output), C is the number of classes, the logarithm is usually natural (i.e., log base e), the sum is only over that index i, where $y_i = 1$, i.e., for the correct class.

Both networks were trained under identical conditions: 100 epochs using backpropagation and three different optimizers (Adam, RMSprop, and SGD), which allowed us to compare not only the structure of the networks but also their sensitivity to the choice of optimization algorithm. To speed up the training process when reaching a plateau, we connected the ReduceLROnPlateau callback, which reduces the training rate if there is no improvement in the loss value for five epochs.

Figure 1 shows a schematic representation of the SMLP architecture, where two layers with the same number of neurons and symmetrical constraints on the weights of the second layer are visible. This highlights the main difference between the two networks and explains the nature of parameter reduction and SMLP's increased resistance to field data noise and reduced computational resource consumption.

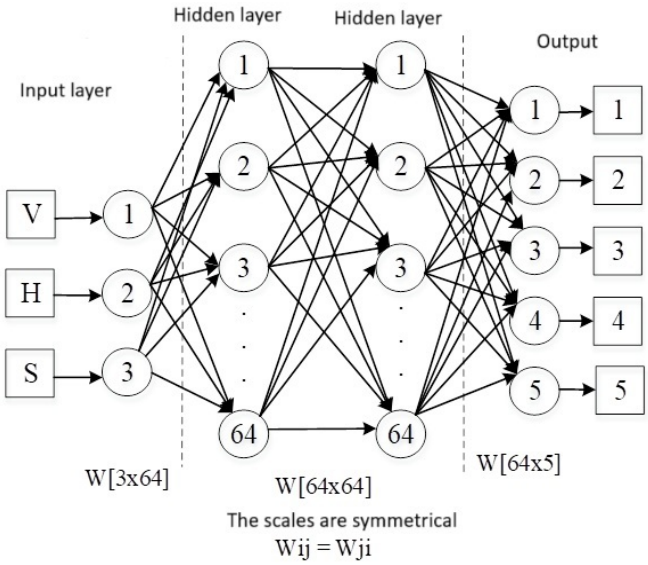

Figure 1. Architecture of the SMLP symmetric network.

III. RESULTS

This section presents a comparative analysis of the experimental results of the standard MLP and its symmetric modification (SMLP) on a test sample, as well as discusses the practical implications of the identified differences. The classification results were evaluated using indicators such as recognition accuracy, area under the ROC curve (AUC), training time and inference time, as well as model stability with different optimizers.

Based on the results of a full run of test data, the standard MLP (see Figure 2) demonstrate an average accuracy of 99.29% and an AUC of 0.9997, while the SMLP (Figure 3) show only a slight decrease in these indicators – to 99.20%

and 0.9996, respectively. Despite the fact that the symmetric approach leads to a reduction in the number of independent parameters in the second hidden layer, the classification quality remained virtually unchanged. This indicates that imposing symmetric constraints does not impair the network's ability to distinguish mine signatures in different soil types.

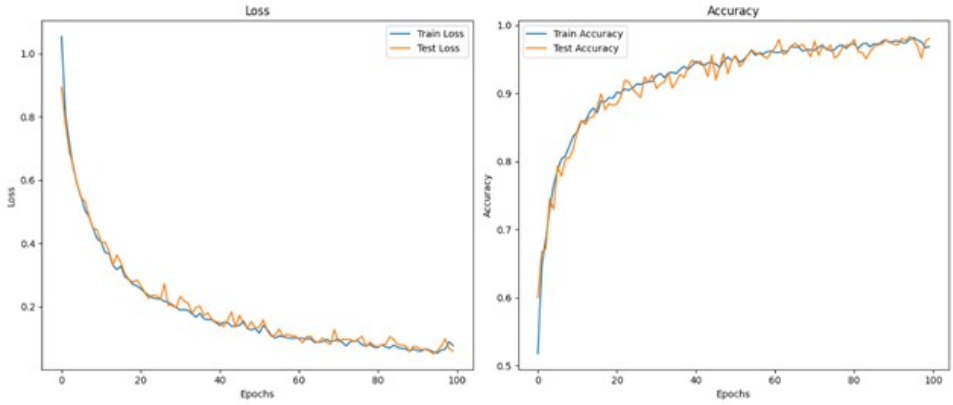

Figure 2. Accuracy and loss graph for SMLP.

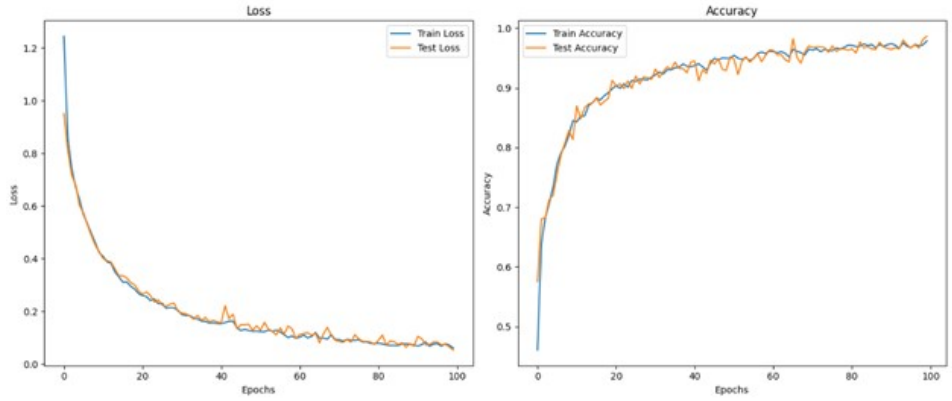

Figure 3. Accuracy and loss graph for MLP.

The most noticeable improvement in SMLP was a reduction in the total training time by almost a third: while training a standard MLP with the Adam optimizer took an average of about 9.2 seconds, SMLP completed training in 6.0 seconds. The reduction in time is explained by the fact that symmetrizing the weights in the second layer reduces the amount of computation during the forward and backward passes through the network. Despite a slight increase in inference time (0.095 s vs. 0.092 s in MLP), this difference is not critical for the task of passive real-time mine detection, as even with symmetry, the network processes all measurements in a fraction of a second. To evaluate suitability for embedded deployment, inference experiments were profiled under CPU-only execution (Intel Core i5 12400F, 16 GB RAM, no GPU acceleration), reflecting resource-constrained environments typical for edge devices. The reported relative reduction in training time (20–30%) corresponds to a proportional decrease in computational operations due to parameter reduction in the symmetric layer. Therefore, the improvement is architecture-driven and hardware-independent.

Special attention should be paid to the behavior of models when using different optimizers. For Adam, the standard MLP and SMLP had accuracies of 99.29% and 99.20%, respectively. When using RMSprop, the difference decreased: SMLP achieved an accuracy of 98.93%, and MLP – 98.40%. This may indicate that a symmetric weight structure increases stability to the choice of optimizer, especially in conditions of an uneven loss landscape. Finally, using SGD, SMLP was more accurate (97.91% vs. 97.64%).

In Figure 4, the graphs show the dependence of loss and accuracy functions for the test sample and demonstrate that SMLP and MLP coincide almost identically.

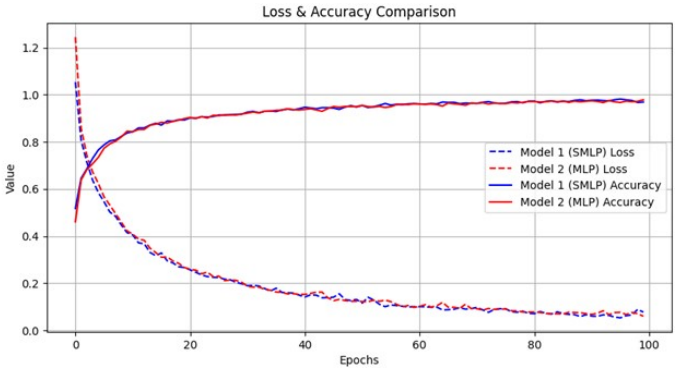

Figure 4. Graphs showing the dependence of loss and accuracy functions on the number of epochs.

Figure 5 shows the ROC (Receiver Operating Characteristic) curves for both models — standard MLP (Model 1) and SMLP (Model 2) — separately for each of the five classes (from 0 to 4). The false positive rate is plotted on the x-axis, and the true positive rate is plotted on the y-axis. The gray dotted line from (0, 0) to (1, 1) corresponds to a

random classifier.

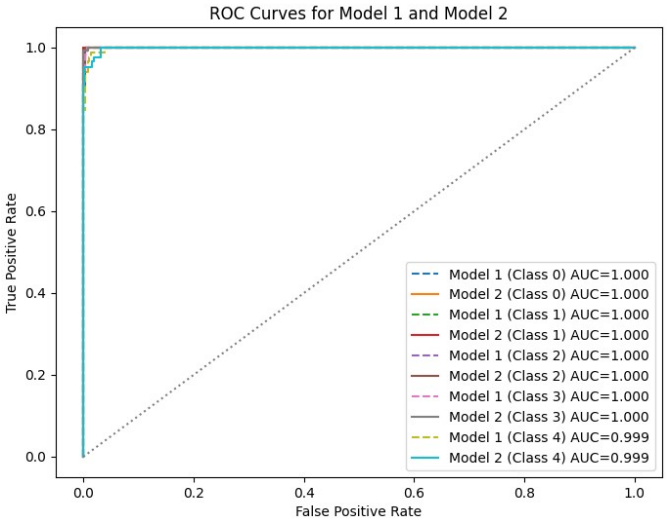

Figure 5. ROC for both MLP and SMLP models.

For classes 0, 1, 2, and 3, both models show absolutely "perfect" curves: they almost merge with the left and upper boundaries of the graph, and the AUC (area under the curve) is 1.000. This means that both MLP and SMLP are able to accurately separate these types of mines from the rest of the signals in the test sample.

For class 4 (the most difficult of the five), the curve is also very close to ideal, but slightly "lags" behind the ideal angle: both models have AUC = 0.999. This indicates a small number of false negatives or false positives in this class, but the accuracy is still exceptionally high.

In general, the graph confirms that the symmetric constraints in SMLP have virtually no effect on the model's ability to distinguish between different types of mines: its ROC curves and AUC are almost identical to those of the standard MLP. This is consistent with previous results, according to which SMLP loses less than 0.09% of accuracy while significantly saving computational resources.

Figure 6 shows the precision and recall dependencies of both models in the form of Precision–Recall curves. Solid lines reflect changes in precision at different classification thresholds, while dotted lines reflect corresponding changes in recall. The red solid curve corresponds to the standard MLP, the blue curve corresponds to the symmetric SMLP, while the red and blue dotted lines illustrate the recall of these same models. Both curves practically do not deviate from the upper limit of the graph, which indicates exceptionally high precision — almost 100% — even at maximum recall. There are practically no significant differences between MLP and SMLP: both models maintain an accuracy of about 1.0 until the completeness drops to unity, and in the last segments of the graph, there are barely noticeable "deviations" of SMLP at the level of thousandths. This means that imposing symmetrical constraints does not affect either the number of missed mines or the number of false positives — both networks demonstrate the same excellent ability to focus on real mine cases. In the context of class unevenness and high sensor noise variability, such stability of Precision–Recall curves confirms the reliability of symmetric architecture for field applications.

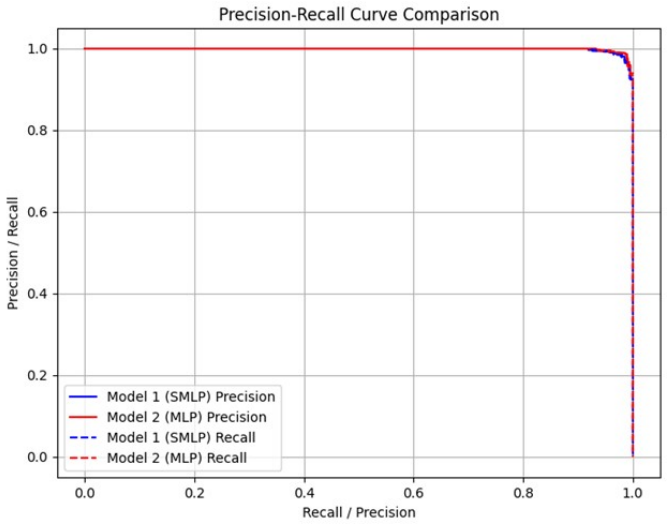

Figure 6. Precision and recall dependencies for both models in the form of Precision–Recall curves.

The confusion matrices of both models (see Figure 7 and Figure 8) clearly show that the overall accuracy of the standard MLP is 0.09% higher than that of the symmetric SMLP, but the nature of the errors in them is different. Let us consider them by class.

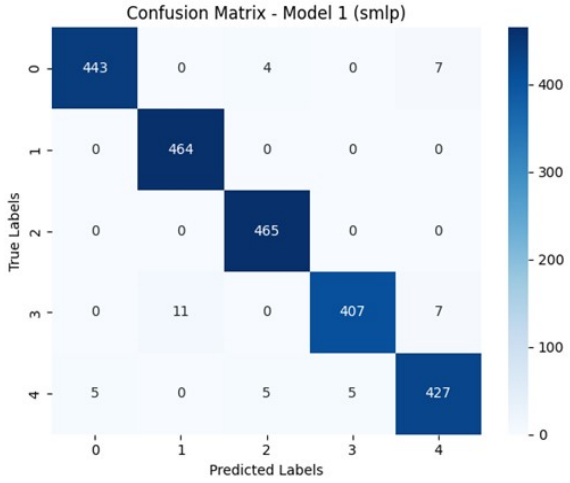

Figure 7. Confusion matrix for SMLP.

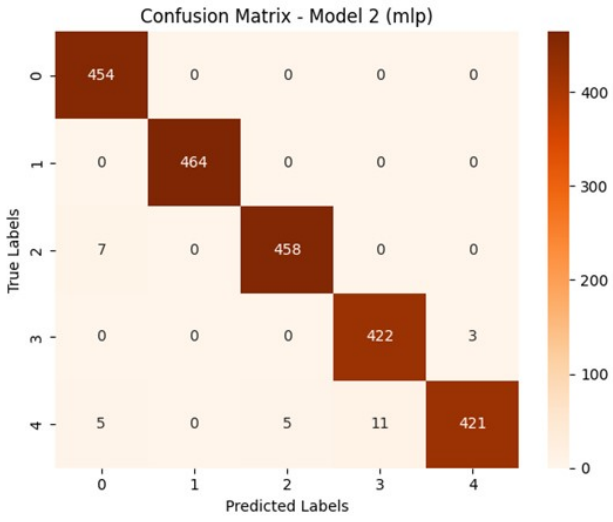

Figure 8. Confusion matrix for MLP.

For class 0, the standard MLP classified all 454 examples correctly, while in SMLP, seven signals were assigned to class 4 and four more to class 2. This means that the imposition of symmetry caused a slight loss of sensitivity to this type, although the absolute accuracy remained extremely high.

In the case of class 1, both networks made no mistakes, indicating the exceptional uniqueness of the characteristics of this type of mine in the dataset.

For class 2, SMLP correctly recognized all 465 test samples, while MLP mistakenly classified seven cases as class 0. That is, for signals of the second type, the symmetric model proved to be even slightly more resistant to false "zeroing."

As for class 3, SMLP made the most errors among all categories: eleven examples were assigned to class 1 and another seven to class 4, while MLP made only three incorrect classifications (all towards class 4). This difference indicates that the symmetric constraint sometimes makes it difficult to clearly distinguish the third type of mines from the others. Class 3 objects exhibit weaker and more irregular magnetic signatures compared to other mine types. Unlike anti-tank or anti-personnel mines that typically contain larger metallic components generating stable and distinguishable magnetic anomalies, booby traps often contain smaller or partially shielded metallic elements. As a result, the voltage response tends to overlap with neighboring classes under varying soil and height conditions. From a modeling perspective, symmetric weight constraints reduce the degrees of freedom in the hidden-to-hidden transformation. While this improves generalization and reduces over-parameterization, it may also slightly limit the network's ability to model asymmetric or highly irregular signal variations. Since class 3 signals demonstrate greater variability and lower amplitude contrast, they become more sensitive to such structural regularization. Therefore, the higher misclassification rate for class 3 does not indicate a structural weakness of the SMLP architecture but rather reflects the intrinsic physical similarity of magnetic responses between certain object types under heterogeneous soil conditions.

Finally, for class 4, SMLP incorrectly labeled five signals as class 0, five as class 2, and another five as class 3. The standard MLP also had five errors in classes 0 and 2, but eleven cases of "spillover" into class 3. Thus, the errors of the two networks were distributed differently: the symmetric MLP gave a little in both directions, while the standard MLP had a greater concentration of errors in the direction of the neighboring class 3.

In total, the standard MLP recorded 31 incorrect predictions against 44 in the SMLP on the same 2250 examples, which corresponds to less than 0.09% difference in overall accuracy. In contrast, the symmetric MLP (SMLP) proved to be somewhat more stable for class 2 and made it possible to reduce the number of synaptic weights between hidden layers by almost half (49,2 %), which significantly saves resources. Such a "redistributed" error does not affect practical mine detection tasks and illustrates how symmetric constraints affect the fine line between the sensitivity and specificity of each class.

When discussing the practical significance of the results obtained, the advantages of SMLP in the context of deployment on embedded platforms should be emphasized. The reduced number of parameters means less memory and computing resources are required, allowing the classification algorithm to be implemented on mobile robots or unmanned aerial vehicles with limited hardware capabilities without losing mine detection accuracy. At the same time, a slight increase in inference time is an acceptable compromise, as the overall data processing speed remains sufficient for real-world use cases.

At the same time, the minimal drop in accuracy (less than 0.09%) shows that symmetry constraints can be applied to optimize the architecture without compromising the final result. However, it should be noted that symmetry constraints on more than one layer or in combination with other hard regularizers can lead to a more significant decline in performance. Therefore, the prospect for further research lies in studying the balance between the degree of symmetry and the depth of the network, as well as in testing the approach on other types of sensor data—for example, a combination of magnetometer and ground-penetrating radar data can be used for mine detection using multimodal neural networks.

Thus, the results confirm that symmetric connections in MLP significantly improve computational efficiency while maintaining high accuracy in detecting mines in different soils. This approach opens up new opportunities for creating portable classifiers with high reliability in field conditions.

The reduction of independent parameters is particularly important for hardware implementation on resource-constrained platforms such as FPGA-based systems. In such architectures, memory footprint and parallel multiply–accumulate operations directly affect power consumption and latency. Therefore, symmetric weight constraints may significantly simplify FPGA deployment and reduce logic utilization.

The study has a number of important advantages that make it relevant for practical applications in the field of passive mine detection. First, the introduction of symmetric constraints in the weight matrices of the second hidden layer allows the total number of synaptic weights between hidden layers to be reduced by almost half (49,2 %), which significantly reduces computational costs during training without a noticeable loss of classification accuracy. This makes it possible to use the developed model on platforms with limited resources — for example, on mobile robots or drones, where every second of training and every megabyte of memory matters. Second, the demonstrated high robustness of SMLP to different optimizers and soil types confirms that the symmetric architecture not only saves resources but also increases the stability of the model in heterogeneous and noisy data conditions. Finally, the versatility of the approach allows it to be integrated into existing signal processing systems without the need to radically change other preprocessing stages or the architecture of the input layer.

At the same time, the study has certain limitations that will be taken into account in our future work. First, symmetric constraints are applied only to synaptic connections between neurons in the first and second hidden layers. Therefore, the question of the scalability of this approach to deeper and more complex architectures, for example with three or more hidden layers, remains open.

In the present study, a shallow architecture (two hidden layers) was intentionally selected due to the low-dimensional and tabular nature of the input features. Increasing network depth in such settings does not necessarily improve performance and may introduce unnecessary parameter

growth and an increased risk of overfitting.

From a theoretical standpoint, the symmetry constraint is not limited to a specific depth. It can be extended to deeper architectures (Deep SMLP) by applying symmetric projections to selected hidden-layer weight matrices. In fact, the relative parameter reduction becomes even more significant as the width and number of hidden layers increase. However, applying symmetry to multiple deep layers may also impose stronger regularization, potentially limiting representational flexibility in highly nonlinear problems and increasing computational requirements.

Therefore, the balance between network depth and structural constraints should be investigated experimentally in future work.

Second, although the inference time increased only slightly (by 0.003 s), the issues of energy consumption and autonomous operation time of mobile platforms during continuous recognition mode should be studied separately, taking into account the hardware limitations of specific devices. Therefore, further steps should focus on adapting symmetric MLP to hybrid multimodal neural networks.

IV. CONCLUSIONS

It is found that the influence of the symmetry of the synaptic connections between the first and second hidden layers in MLP turned out to be decisive: imposing symmetric constraints on the connections between the first and second hidden layers allows us to significantly reduce the number of independent parameters (almost twice), while maintaining high accuracy of the mine recognition model in soils of different structures. At the same time, the number of weighted connections between neurons in the two-layer block is reduced by almost 50%, which leads to a reduction in memory size and acceleration of the learning process by 20–30% (9,2 s – MLP; 6,0 s – SMLP) without a noticeable loss of accuracy.

Despite the reduction in the number of parameters, the SMLP demonstrates an average accuracy of 99.20% and AUC 0.9996, which is practically no different from the results of the traditional MLP network - 99.29% and AUC 0.9997. In addition, SMLP shows less sensitivity to the choice of optimizer - an important property when working with heterogeneous soils.

Experimentally proven results show that the reduced computational complexity makes SMLP promising for implementation in systems with limited resources – mobile robots, drones and other autonomous platforms. Although the time of one inference in SMLP is 0.095 s versus 0.092 s in standard MLP, SMLP remains acceptable for real-time tasks.

Thus, symmetrizing the connections between hidden layers of MLP is an effective method for optimizing the mine classifier: it combines high accuracy with reduced hardware requirements, opening up new opportunities for creating portable and reliable passive mine detection systems.

References

[1] Landmine Monitor Report, The Monitor, 2024. [Online]. Available at: https://the-monitor.org/reports/landmine-monitor-2024.

[2] M. Šimić, D. Ambruš, and V. Bilas, "Landmine identification from pulse induction metal detector data using machine learning," *IEEE Sensors Letters*, vol. 7, pp. 1–4, 2023, https://doi.org/10.1109/LSENS.2023.3307091.

[3] H. Liu, C. Zhao, J. Zhu, J. Ge, H. Dong, Z. Liu, and N. Mrad, "Active detection of small UXO-like targets through measuring electromagnetic responses with a magneto-inductive sensor array," *IEEE Sensors Journal*, vol. 21, pp. 23558–23567, 2021, https://doi.org/10.1109/JSEN.2021.3107842.

[4] M. Munschy, D. Boulanger, P. Ulrich, and M. Bouiflane, "Magnetic mapping for the detection and characterization of UXO: Use of multi-sensor fluxgate 3-axis magnetometers and methods of interpretation," *Journal of Applied Geophysics*, vol. 61, pp. 168–183, 2006, https://doi.org/10.1016/j.jappgeo.2006.06.004.

[5] A. Barnawi, K. Kumar, N. Kumar, B. Alzahrani, and A. Almansour, "A deep learning approach for landmines detection based on airborne magnetometry imaging and edge computing," *Computer Modeling in Engineering & Sciences*, vol. 139, pp. 2117–2137, 2023, https://doi.org/10.32604/cmes.2023.044184.

[6] *D. Jafuno, A. Mian, G. Ginolhac, and N. Stelzenmuller*, "Classification of buried objects from ground penetrating radar images using second order deep learning models," *IEEE Journal of Selected Topics in Applied Earth Observations and Remote Sensing*, vol. 18, pp. 3185–3197, 2025, https://doi.org/10.1109/JSTARS.2024.3524424.

[7] C. Yılmaz, Y. Sönmez, H. T. Kahraman, S. Soyler, and U. Güvenç, "Developing of decision support system for land mine classification by meta-heuristic classifier," *Proceedings of the International Symposium on Innovations in Intelligent Systems and Applications (INISTA)*, Sinaia, Romania, 2016, pp. 1–5, https://doi.org/10.1109/INISTA.2016.7571867.

[8] J. Amarel, C. Rudolf, A. Iliopoulos, J. Michopoulos, and L. N. Smith, "Symmetry constrained neural networks for detection and localization of damage in metal plates," arXiv preprint, 2024, https://doi.org/10.1063/5.0242345.

[9] S. N. M. Kanafiah et al., "Metal shape classification of buried object using multilayer perceptron neural network in GPR data," *IOP Conf. Series: Materials Science and Engineering*, vol. 705, Art. no. 012028, 2019, https://doi.org/10.1088/1757-899X/705/1/012028.

[10] Y. Wang, X. Ma, Z. Chen, Y. Luo, J. Yi, and J. Bailey, "Symmetric cross entropy for robust learning with noisy labels," *Proceedings of the IEEE/CVF Int. Conf. Computer Vision (ICCV)*, 2019, pp. 322–330, https://doi.org/10.1109/ICCV.2019.00041.

[11] J. Vyhnanek, M. Janoseka, and P. Ripka, "AMR gradiometer for mine detection and sensing," *Procedia Engineering*, vol. 25, pp. 362–366, 2012, https://doi.org/10.1016/j.proeng.2011.12.089.

[12] Z. Wen, S. Han, C. Gao, Y. Chen, L. Guo, and Y. Zhang, "A deep learning method for recognizing types of unexploded ordnance based on magnetic detection," *IEEE Transactions on Geoscience and Remote Sensing*, vol. 62, pp. 1–13, 2024, Art. no. 5918313, https://doi.org/10.1109/TGRS.2024.3405478.

[13] S. A. Stankevich and I. Y. Saprykin, "Optical and magnetometric data integration for landmine detection with UAV," *WSEAS Transactions on Environment and Development*, vol. 20, pp. 1059–1066, 2024, https://doi.org/10.37394/232015.2024.20.96.

[14] I. Poliachenko, V. Kozak, V. Bakhmutov, S. Cherkes, and T. Bilyi, "Exploratory study of potential applications of UAV magnetic surveys for unexploded ordnance detection in coastline zone," *Geofizicheskiy Zhurnal*, vol. 47, no. 1, 2025, https://doi.org/10.24028/gj.v47i1.316760.

[15] X. Zhou, Z. Chen, H. Chen, S. Wang, and Z. O. Kubeka, "Edge detection of source body from magnetic anomaly based on ResNet," *Remote Sensing*, vol. 16, Art. no. 4139, 2024, https://doi.org/10.3390/rs16224139.

[16] M. F. Işık, Ç. Suiçmez, and C. Yılmaz, "Low-cost mine detector design using magnetic anomaly method," *Politeknik Dergisi*, vol. 25, no. 4, pp. 1729–1740, 2022. https://doi.org/10.2339/politeknik.1080410.

[17] H. Huang and I. J. Won, "Characterization of UXO-like targets using broadband electromagnetic induction sensors," *IEEE Transactions on Geoscience and Remote Sensing*, vol. 41, no. 3, pp. 652–663, 2003, https://doi.org/10.1109/TGRS.2003.809936.

[18] H. Tanaka and D. Kunin, "Noether's learning dynamics: Role of symmetry breaking in neural networks," Proceedings of the 40th International Confereence on Machine Learning (ICML), 2023.

[19] X. S. Hu, S. Zagoruyko, and N. Komodakis, "Exploring weight symmetry in deep neural networks," *Computer Vision and Image Understanding*, vol. 187, 2019, https://doi.org/10.1016/j.cviu.2019.07.006.

[20] G. Zhou and S. Reichle, "UAV-based multi-sensor data fusion processing," *International Journal of Image and Data Fusion*, vol. 1, no. 3, pp. 283–291, 2010, https://doi.org/10.1080/19479832.2010.497343.

[21] B. Rusyn, O. Lutsyk, R. Kosarevych et al., "Rethinking deep CNN training: A novel approach for quality-aware dataset optimization," *IEEE Access*, vol. 12, pp. 137427–137438, 2024, https://doi.org/10.1109/ACCESS.2024.3414651.

[22] B. Rusyn, O. Lutsyk, R. Kosarevych et al., "Features extraction from spectral remote sensing images based on multi-threshold binarization," *Scientific Reports*, vol. 13, no. 1, Art. no. 19655, 2023, https://doi.org/10.1038/s41598-023-46785-7.

[23] K. D. G. Maduranga, V. Zadorozhnyy, and Q. Ye, "Symmetry-structured convolutional neural networks," *Neural Computing and Applications*, vol. 35, pp. 4421–4434, 2022, https://doi.org/10.1007/s00521-022-08168-3.

[24] K. D. G. Maduranga, V. Zadorozhnyy, and Q. Ye, "Symmetry-structured convolutional neural networks," Neural Computing and Applications, vol. 35, pp. 4421–4434, 2023, https://doi.org/10.1007/s00521-022-08168-3.

[25] R. Peleshchak, V. Lytvyn, O. Mediakov, and I. Peleshchak, "Morphology of convolutional neural network with diagonalized pooling," in *Communications in Computer and Information Science*, 2023, pp. 161–172, https://doi.org/10.1007/978-3-031-27034-5_11.

[26] X. S. Hu, S. Zagoruyko, and N. Komodakis, "Exploring weight symmetry in deep neural networks," arXiv preprint, 2018, doi: 10.48550/arXiv.1812.11027.

[27] R. Agrawal and J. Pradeep, "Land mines detection," Kaggle Dataset, 2020. [Online]. Available at: https://www.kaggle.com/datasets/ritwikb3/land-mines-detection.

ROMAN PELESHCHAK, *Doctor of Physical and Mathematical Sciences, Professor, Department of Information Systems and Networks, Lviv Polytechnic National University.*
Research interests: computer science, artificial intelligence, machine learning, neural networks, image processing, pattern recognition, solid state physics, theoretical physics.
E-mail: roman.m.peleshchak@lpnu.ua
ORCID: https://orcid.org/0000-0002-0536-3252

VASYL LYTVYN, *Doctor of Technical Sciences, Professor, Department of Information Systems and Networks, Lviv Polytechnic National University.*
Research interests: computer science, models of computation, theory of computation, mathematics of computing, analysis of algorithms, computer systems, software engineering, software development, artificial intelligence, neural networks.
E-mail: vasyl.v.lytvyn@lpnu.ua
ORCID: https://orcid.org/0000-0002-9676-0180

DMYTRO DOSYN, *Doctor of Technical Sciences, Professor, Head of the Department of Information Systems and Networks, Lviv Polytechnic National University.*
Research interests: computer science, intelligent systems, artificial intelligence, data analysis, distributed systems, automated planning, social network analysis, biometric authentication.
E-mail: dmytro.h.dosyn@lpnu.ua
ORCID: https://orcid.org/0000-0003-4040-4467

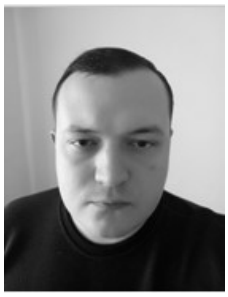

IVAN PELESHCHAK, *PhD 124 System analysis, Department of Information Systems and Networks, Lviv Polytechnic National University.*
Research interests: computer science, artificial intelligence, machine learning, neural networks, image processing, signal processing, pattern recognition, data analysis.
E-mail: ivan.r.peleshchak@lpnu.ua
ORCID: https://orcid.org/0000-0002-7481-8628

TARAS BATIUK, *PhD 124 System analysis, Department of Information Systems and Networks, Lviv Polytechnic National University.*
Research interests: computer science, artificial intelligence, machine learning, natural language processing, text mining, sentiment analysis, social network analysis, intelligent systems.
E-mail: taras.m.batiuk@lpnu.ua
ORCID: https://orcid.org/0000-0001-5797-594X.